JACS
JOURNAL OF THE AMERICAN CHEMICAL SOCIETY
Article
pubs.acs.org/JACS

Detection of Specific Protein−Protein Interactions in Nanocages by Engineering Bipartite FlAsH Binding Sites

Thomas A. Cornell,[†,‡] Jing Fu,[‡,∥] Stephanie H. Newland,[§,∥] and Brendan P. Orner[†,*]

[†]Department of Chemistry, King's College London, London, SE1 1DB, United Kingdom
[‡]Division of Chemistry and Biological Chemistry, Nanyang Technological University, Singapore, 637371
[§]School of Chemistry, University of Southampton, Southampton, SO17 1BJ, United Kingdom

Supporting Information

ABSTRACT: Proteins that form cage-like structures have been of much recent cross-disciplinary interest due to their application to bioconjugate and materials chemistry, their biological functions spanning multiple essential cellular processes, and their complex structure, often defined by highly symmetric protein−protein interactions. Thus, establishing the fundamentals of their formation, through detecting and quantifying important protein−protein interactions, could be crucial to understanding essential cellular machinery, and for further development of protein-based technologies. Herein we describe a method to monitor the assembly of protein cages by detecting specific, oligomerization state dependent, protein−protein interactions. Our strategy relies on engineering protein monomers to include cysteine pairs that are presented proximally if the cage state assembles. These assembled pairs of cysteines act as binding sites for the fluorescent reagent FlAsH, which, once bound, provides a readout for successful oligomerization. As a proof of principle, we applied this technique to the iron storage protein, DNA-binding protein from starved cells from *E. coli*. Several linker lengths and conformations for the presentation of the cysteine pairs were screened to optimize the engineered binding sites. We confirmed that our designs were successful in both lysates and with purified proteins, and that FlAsH binding was dependent upon cage assembly. Following successful characterization of the assay, its throughput was expanded. A two-dimension matrix of pH and denaturing buffer conditions was screened to optimize nanocage stability. We intend to use this method for the high throughput screening of protein cage libraries and of conditions for the generation of inorganic nanoparticles within the cavity of these and other cage proteins.

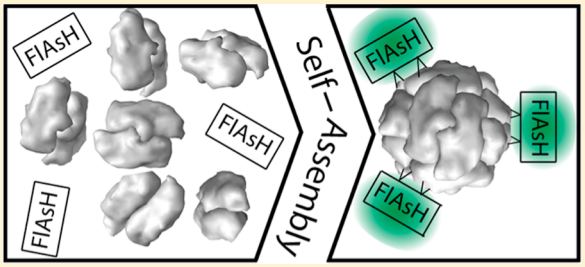

INTRODUCTION

Large, hollow, and often symmetric, cage-like protein assemblies, like ferritin nanocages and virus capsids, provide impetus for investigations into protein folding, protein−protein interactions, and self-assembly, all of which underpin protein quaternary structure.[1−3] On a biofunctional level, similar protein nanostructures are involved in sequestering metals,[4] creating size-specific pockets of a hydrophobic environment to assist in protein folding,[3] catalyzing the generation of metabolites,[5] as well as delivering and protecting viral genomes.[6] Along with having fundamental importance, protein cages have been the focus of much applied research. To date, protein cages have been used as size constraining reaction vessels for the construction of inorganic materials, and for several potential biomedically relevant applications such as drug and siRNA delivery.[7−13]

Many high resolution protein cage structures are available.[14,15] These structures have paved the way for rational engineering and design, a pursuit that is important for enhancing the properties of protein cages to match those required for further applications. One successful design strategy, applied in different ways, has been to enhance the protein−protein interactions between monomers.[16−19] However, this type of research can be protracted due to the necessity of iteratively purifying each mutant followed by extensive biophysical characterization with techniques that are often not directly related to cage formation.[2,20]

Ferritins are ubiquitous protein cages whose structure has been extensively studied due to its relatively straightforward folding and assembly. They store cellular iron through mineralization inside their hollow cavity. *E.coli* DNA-binding protein from starved cells (Dps), a mini-ferritin, has a 9 nm outer diameter and assembles from twelve identical monomers.[21−26] Each monomer folds into a four-helix bundle with an additional helix along the loop between the second and third helix of the bundle (the "BC helix").[17,27] During ferritin self-assembly, monomers rarely persist and for most ferritins, a 2-fold symmetric dimer is believed to be the most prevalent intermediate. This dimer is thought to be the fundamental building block for cage formation.[21] In Dps, these intermediates are most likely antiparallel dimers. A consequence of this is that the termini of each monomer projects away from those of the other monomer; only with increased oligomerization to the

Received: August 16, 2013
Published: October 8, 2013

   dx.doi.org/10.1021/ja4085034 | J. Am. Chem. Soc. 2013, 135, 16618−16624

fully formed cage state do the termini converge. Although ferritins have been pursued extensively for applications in material science,[10] only minimal work has been performed to optimize the properties of the ferritins for these applications.

Unfortunately, there are few methods for determining the oligomerization states of the cages other than expressing, purifying and assaying each protein followed by mostly low throughput biophysical techniques, such as size exclusion chromatography (SEC), dynamic light scattering (DLS), and transmission electron microscopy (TEM).[2,16,17,20,28] Creating a system that can rapidly identify specific oligomerization states *in vivo* or in cell lysates, would greatly advance research on protein nanocages and protein self-assembly in general.

An ideal method would be one that could distinguish specific protein−protein interactions during the assembly process. A direct oligomerization assay employing a biarsinical fluorescent reagent,[29,30] of which FlAsH and ReAsH are the most common, is one possibility. These reagents, which have been used as an alternative to GFP variants for protein labeling,[31−34] exploit the affinity of their arsenic atoms for sulfur atoms in a protein. The reagents bind selectively to proteins with four appropriately presented cysteines (Supporting Information, SI, Figure S1). This binding results in fluorescence most likely due to a change in rotational properties about the carbon−arsenic bond.[35,36] Originally, it was suggested that FlAsH ideally interacts with cysteines displayed on a single face of an α-helix, but later it was shown that the sequence CCPGCC provides an ideal FlAsH binding site.

Recently, it has been shown that the four cysteines in the FlAsH binding motif can be split into two "bipartite" cysteine pairs. If the two pairs are positioned apart from each other in the polypeptide sequence, then FlAsH can be used to detect when they become proximal during protein folding. Similarly, the two pairs can be placed on two separate polypeptides, and FlAsH can be used to monitor the formation of a protein−protein interaction if the cysteines are positioned appropriately across the interface.[35,37,38] Recently this strategy was used to elucidate conformationally transduced signals through the cellular membrane and to provide an explanation for the divergent signaling outcomes of an EGF receptor that dimerizes through coiled-coil motifs.[39]

The first step in developing the biarsinical reagents into probes for protein cage assembly is to design binding sites that only appear upon cage formation. This goal is made more challenging by the fact that the monomers of protein cages, such as Dps, use multiple interfaces for cage formation and various states could be intermediates along the oligomerization pathway. Thus, a design with ultimate utility would be robust enough to distinguish between these oligomerization states. One possible solution therefore would be to design ferritin binding sites that exploit the divergence of monomer termini in the antiparallel dimer intermediate (see above). In the cage form, these termini converge. Thus, terminally appended cysteines would provide a sulfur-rich area for a FlAsH binding site that only forms upon cage assembly and not in a dimer intermediate. One must also consider the location of native cysteine residues. Dps has a single native cysteine that is 23 Å from the corresponding cysteine in the nearest monomer when assembled into a cage (SI Figure S2). While this will not impede this investigation, consideration must be taken when applying this approach to other proteins.

In our design, we placed cysteine pairs at the Dps C-terminus. (Figure 1) A series of mutants were generated to optimize the binding site; these mutants differ in how the two cysteines are displayed by the monomer either based on linker length (**DpsCC**, **DpsGCC**, **DpsGGCC**, **DpsGGGCC**) or conformation (**DpsPAGCC**). (Figure 2a) Extending the C-terminus to display the peptide sequence CCPGCC which includes all four cysteines of an ideal binding site on a single monomer (see above) resulted in the positive control (**DpsCCPGCC**), which would require neither folding nor assembly to generate a FlAsH signal. We used wild-type Dps, which has no additional cysteines, as a negative control (**Dps**).

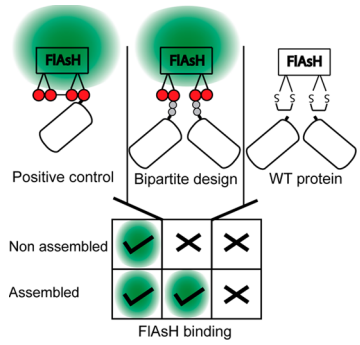

Figure 1. Fluorescence (green) from the reagent FlAsH, is assembly state dependent only in the bipartite design because of the need to have two sets of cysteine pairs (red) to form a binding site. The positive control provides a binding site that is neither folding, nor oligomerization dependent, whereas the negative control provides no FlAsH binding. This is the basis of our strategy to directly monitor protein cage formation.

RESULTS AND DISCUSSION

An oligomerization state assay with the most utility would be able to evaluate multiple samples rapidly. Therefore, instead of initially working with purified proteins, we used cellular lysates. This decision increased our throughput, allowing the screening of more potential designs. In addition, the use of complex solutions allowed us to screen for selectivity and the success of this method in lysates would demonstrate specificity in the presence of metal ions and sulfur containing metabolites and proteins. We employed conditions containing 1,2-ethanedithiol (EDT), 2-mercaptoethanol (2-ME), tris(2-carboxyethyl)-phosphine (TCEP), and ethylenediaminetetraacetic acid (EDTA) to control oxidation state and metal ion concentration consistent with the literature,[29,30,37,38] however, our conditions are not fully optimized. In lysates, (Figure 2b) the positive control, **DpsCCPGCC**, generated robust fluorescence with added FlAsH, and the negative control (**Dps**) gave nearly undetectable signal. Of the bipartite designs, **DpsCC** and **DpsGCC** had a very weak response, whereas **DpsGGCC**, **DpsGGGCC**, and **DpsPAGCC** gave fluorescence that was between 15 and 35% of the positive control, suggesting that a longer linker is ideal, and one that is more rigid may be optimal.

To confirm that the FlAsH binding is indeed dependent on cage formation, we subjected the lysates to similar experiments but in denaturing conditions. (Figure 2c) As expected, the negative control, **Dps**, exhibited no change in fluorescence upon denaturation.

The positive control, **DpsCCPGCC**, was also expected to have no change, however, it did generate a small, but significant loss, which may be attributed to restricted access to the tetracysteine tag in the cage and may be suggestive that more optimized equilibration times could enhance the assay. As

dx.doi.org/10.1021/ja4085034 | J. Am. Chem. Soc. 2013, 135, 16618−16624

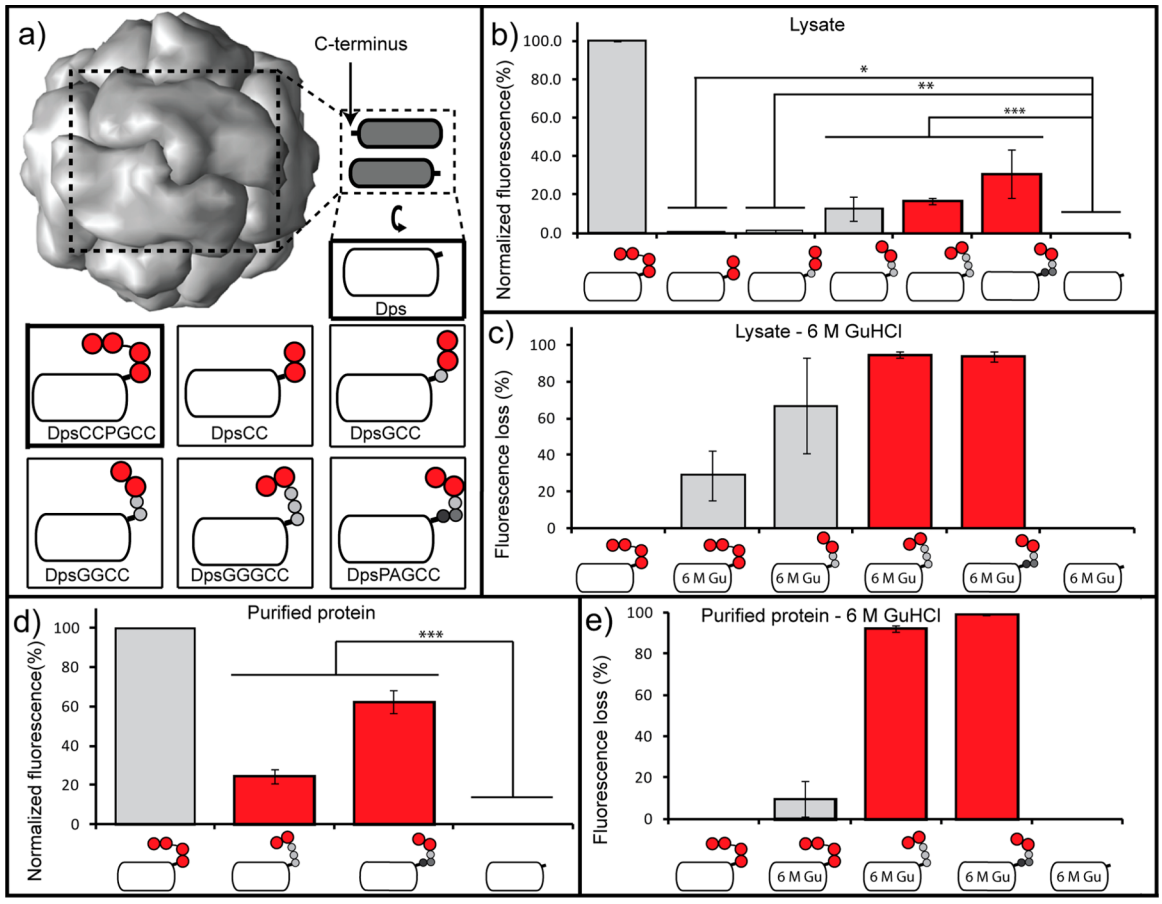

Figure 2. (a) Dps crystal structure (PDB: 1DPS) emphasizing a dimer subunit and divergent presentation of the C-termini along with schematics representing proteins used in this study. The negative control (Dps) has no appended C-terminal cysteines whereas the monomer of the positive control (DpsCCPGCC) displays a full binding site. The other proteins present a pair of cysteines with a variety of flexible and constrained linkers. Cysteine (red), glycine (light gray), alanine (dark gray), and proline (black). (b) FlAsH fluorescence, normalized to controls, for the proteins overexpressed as cell lysates diluted to the same total protein concentration (0.1 mg/mL). (c) Percent fluorescence loss for the proteins in lysates in denaturing conditions. (d) FlAsH fluorescence, normalized to controls, for the proteins overexpressed and purified, diluted to the same protein concentration (0.1 mg/mL). (e) Percent fluorescence loss for the purified proteins in denaturing conditions. The lysate and purified protein data are from six and eight replicates, respectively. Error bars are SD * Two-tailed *P*-values = 0.4804. ** Two-tailed *P*-values = 0.020 050. *** Two-tailed *P*-values = 0.0001.

expected, the bipartite designs displayed a large loss in fluorescence upon denaturation with **DpsGGGCC** and **DpsPAGCC** exhibiting a nearly 100% loss in signal with added denaturant. To verify these results, the leading proteins were expressed, purified (SI Figure S11 for sequencing data), and fully characterized (SI Figures S4−S8 and SI Table S4 for gels and mass spec, SEC, TEM, CD) and were subjected to the binding experiment and subsequent denaturation. (Figure 2d,e) Again, the controls behaved as expected with the exception of the positive control that, again, lost a small amount of signal upon denaturation.

The bipartite designs, **DpsGGGCC** and **DpsPAGCC**, displayed strong, oligomerization-dependent binding of FlAsH with the latter generating ∼50% of control. It should be noted that the bipartite mutants halve the number of cysteine residues and therefore would be expected to have fewer available binding sites per protein, but, with that stated, we have not yet rigorously established saturation stoichiometry. These data again demonstrate that at least one binding site design was successful and that our "quick and dirty" lysate-based screen generates accurate results, indicating the potential for further optimization and expanding the throughput.

The steady state fluorescence experiments, coupled with denaturation, strongly demonstrate that we have successfully designed FlAsH binding sites that are oligomerization dependent. While those experiments, combined with the geometrical placement of the binding sites, suggested that this dependence is specific to the cage state over the dimer state, it needed to be directly confirmed. We have previously shown that some ferritins can exist in solution as mixtures of cage and dimer through the use of SEC.[28] Therefore we employed SEC, combining protein absorbance (280 nm) with FlAsH fluorescence (535 nm). If the binding sites were successfully designed to appear during the formation of specific protein−protein interactions, then fluorescent peaks should correspond to only certain oligomerization forms. (Figure 3) The negative control, **Dps**, which is a wild-type protein we have worked with extensively, generates a single peak from the cage and no detectable dimer when monitored at 280 nm (Figure 3b). Also as expected, no peak is observed in the FlAsH channel. For the positive control, **DpsCCPGCC**, a cage and a small dimer peak at 280 nm are observed, and the fluorescence elutes with both, again as expected, indicating no preference for oligomerization state. (Figure 3a) The proteins with the bipartite binding sites,

dx.doi.org/10.1021/ja4085034 | J. Am. Chem. Soc. 2013, 135, 16618−16624

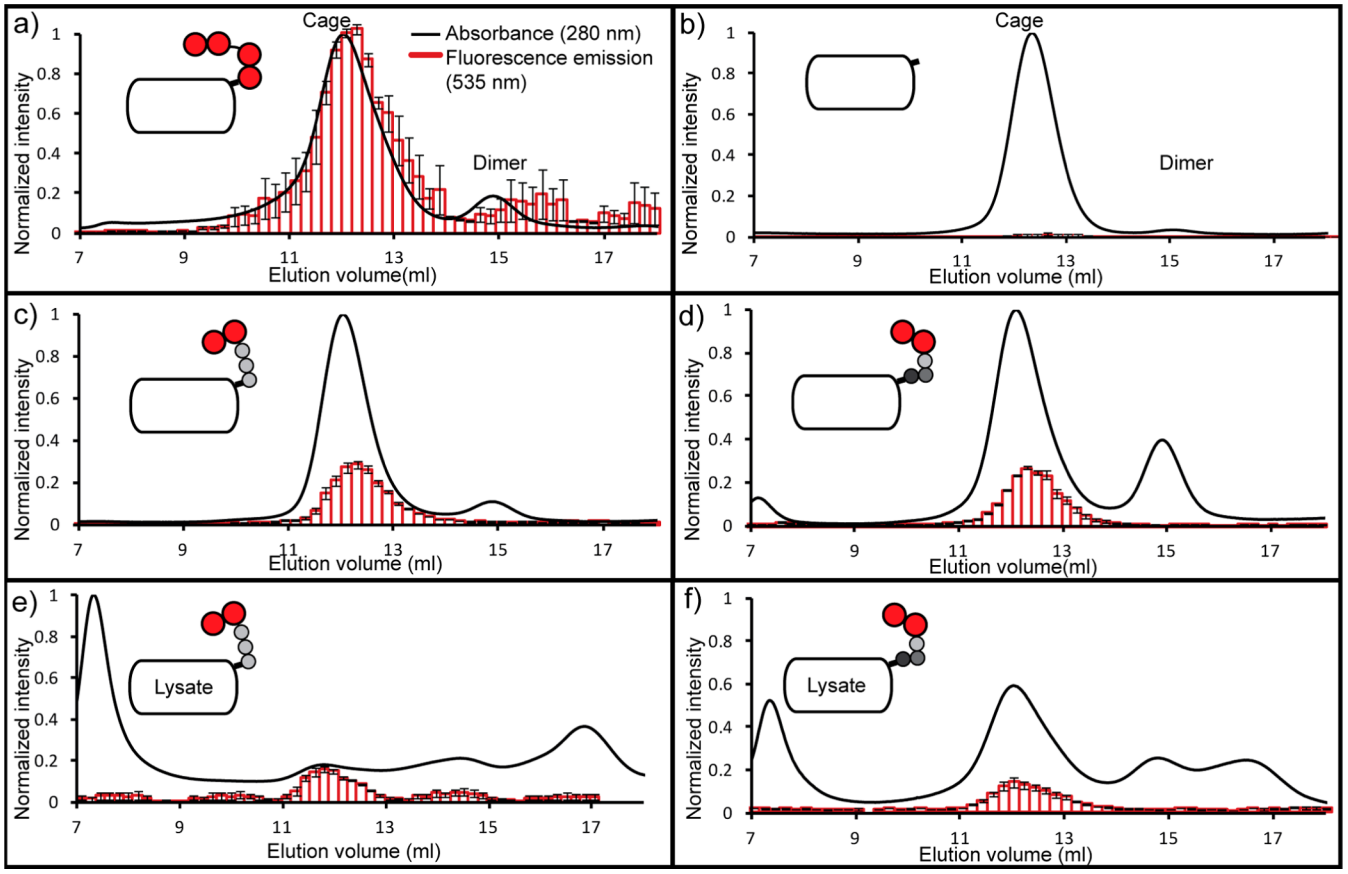

Figure 3. Size exclusion chromatograms monitored at absorbance of 280 nm (protein) and fluorescence at 535 nm (bound FlAsH) to determine if the assay is selective for the cage oligomerization state. (a–d) Purified proteins (0.5 mL injection of 1 mg/mL). (e,f) Lysate solutions with overexpressed designed protein (0.5 mL injection of 1 mg/mL total protein). All absorbance and fluorescence signals are normalized to the positive control. Results for both the UV and fluorescence traces are averages of three runs. Error bars are SD.

DpsPAGCC and **DpsGGGCC**, both show a cage and a dimer peak at 280 nm, however, the fluorescence only elutes with the cage, suggesting that the designed binding sites are forming only upon cage formation and that this assay can distinguish between oligomerization states (Figure 3c,d). It should be noted that **DpsPAGCC** did slightly aggregate. The fact that the aggregate peak also had no fluorescence further demonstrates the robustness of this approach. As a further test of specificity, the same technique was used to assess clarified lysates for **DpsPAGCC** and **DpsGGGCC** (Figure 3e,f). Again, fluorescence elutes at a volume consistent with the cage state. Taken together, these data strongly suggest that not only are the designed binding sites forming upon oligomerization, but also they form only upon cage formation.

An additional goal of this technique is not only to develop a direct screen for specific oligomerization states of protein cages, but also to expand the throughput of this characterization. Therefore it was modified to a 96-well plate format. As a proof of principle, but also as a means to optimize our work with these proteins (see above), we sought to discover conditions of highest stability. First we expanded our denaturation experiment described in Figure 1 to screen a variety of denaturant concentrations. (Figure 4a) As expected, and consistent with our previous data, the positive control, **DpsCCPGCC**, generated high signal at all conditions, demonstrating that FlAsH binding is not oligomerization dependent. The negative control, **Dps**, generates no signal across all conditions. However, a protein with the designed bipartite binding site,

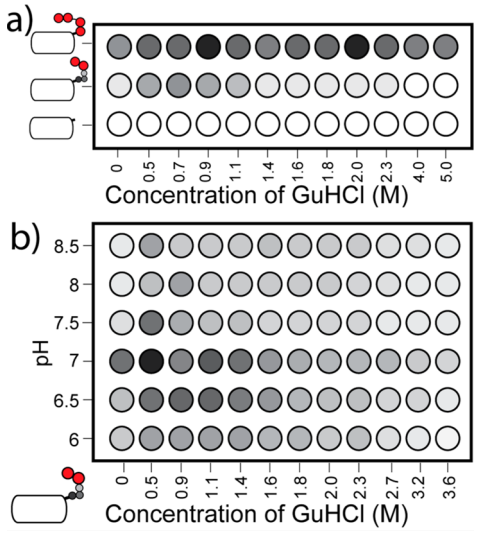

Figure 4. Medium throughput screen of buffer conditions favoring cage oligomerization state. Fluorescence intensity is grayscaled so that black is most intense and white is least. (a) Normalized fluorescence intensity of **DpsCCPGCC**, **DpsPAGCC**, and **Dps** as a function of GuHCl concentration at pH 7.8. Values are the average of at least six replicates. SD is included in SI Figure S10. (b) Normalized fluorescence intensity for **DpsPAGCC** as a function of both pH and GuHCl. Values are averages of three replicates. SD is included in SI Figure S9.

dx.doi.org/10.1021/ja4085034 | J. Am. Chem. Soc. 2013, 135, 16618–16624

DpsPAGCC, loses its ability to bind FlAsH near 1.4 M denaturant. (SI Figure S10)

Further expanding our enquiry into ideal conditions for Dps stability, we screened both denaturant and pH concurrently. (Figure 4b and SI Figure S9) It should be noted that, consistent with most of the literature,[35,37] we usually perform our experiments with Dps at pH 7.8. Thus, it was somewhat surprising to discover that the protein is most stable below pH 7.0. These experiments would have been less possible in lower throughput screens, as they would have taken longer and expended a large amount of reagents. This not only emphasizes the strength of this approach in that its throughput can be expanded, but also this increased throughput can lead to useful experiments (with potentially unexpected results) that may not have been run due to the exigent nature of traditional techniques.

CONCLUSIONS

Protein cages have the potential for applications in fields as wide spanning as drug delivery, catalysis, and nanomaterials. Moreover, they can act as model systems to study biologically ubiquitous protein−protein interactions, self-assembly and quaternary structure, all of which are at the cutting edge of pharmaceutical interest. However, for protein cages to reach their full potential, tools to assess directly their solution assembly properties in higher throughput are necessary. By engineering FlAsH binding sites and protein−protein interfaces that only form in the cage oligomerization state and not in the presumed dimer intermediate, we designed a system to directly detect assembly in cellular lysates of the miniferritin *E. coli* Dps. We have shown that indeed this system is oligomerization-dependent and is specific for the cage and not the dimer. In addition, we demonstrated the scalability of this system by performing a two-dimensional, medium throughput screen to determine conditions that favor the cage state. We are currently expanding this technique to other ferritins in the form of protein libraries screened in whole bacteria for the purpose of discovering "switchable" protein cages and those with bespoke properties for specific applications like nanoparticle formation while optimizing the designs based on ideal binding sites.[38,40] In addition, we are intending to use this technique to target specific oligomerization states in order to monitor their formation along the self-assembly pathway. We believe that this strategy can be easily ported to other protein cages and self-assembling protein systems in order to optimize their properties and to understand their formation.

MATERIALS AND METHODS

FlAsH Binding in Lysates. The pET-22b expression vectors containing Dps design variants (SI Methods and materials S1 for cloning information) were transformed into Rosetta *E. coli* cells (Novagen) and plated on LB agar plates (50 μL/mL of carbenicillin and 34 μL/mL chloramphenicol). Selected colonies then were grown in LB (3 mL of 50 μL/mL of carbenicillin, 37 °C, overnight) as a preculture which was then added to LB (100 mL) and grown (37 °C) to an $O.D_{600}$ of 0.6. Protein expression was then induced by the addition of IPTG (50 μL of a 1 M stock) and the culture was further incubated (3 h, 30 °C). The cells were isolated by centrifugation (4000 rpm, 15 min at 4 °C). The cell pellet was resuspended in FlAsH buffer (100 mM Tris·HCl, 100 mM NaCl, 1 mM EDTA, pH 7.8) and sonicated (Misonix, Ultrasonic cell disruptor, pulsed 5 s on, 5 s off for 5 min). The protein solution was clarified by centrifugation (15 000 rpm, 45 min, 4 °C) and then filtered (Sartorius, 0.2 μm).

The protein concentration was determined (BCA, Novagen) and the cell lysate was diluted to 1 mg/mL with FlAsH buffer. To ensure that all the 1 mg/mL samples had similar amounts of the desired protein, each was analyzed by SDS PAGE (SI Figure S3). Each fluorescence experiment contained protein lysate (200 μL, 0.1 mg/mL) in FlAsH buffer, TCEP (Sigma, final concentration of 3.5 mM), EDT (Sigma, final concentration of 1 mM) and 2-ME (Sigma, final concentration of 1 mM) were added, and the solution was incubated (room temperature, 2 h) followed by the addition of FlAsH-EDT_2 (Invitrogen, final concentration of 0.1 μM) followed by a further incubation (room temperature, 2 h) in the dark. Each lysate sample was tested in a black Corning 96 well plate in a PerkinElmer Envision 2101 multilabel plate reader, with each design being expressed three times and each expression being tested in 6 different wells and re read twice (Ex filter 485 nm, bandwidth 14 nm, Em filter 535 nm, bandwidth 25 nm). For the denatured experiments, the above was repeated but with the extra addition of 6 M guanidine and incubated for 2 h prior to the addition of TCEP, EDT, and 2-ME, with the protein concentration remaining the same as in previous undenatured experiments.

FlAsH Binding with Purified Proteins. The pET-32b vectors containing the Dps variants (SI Methods and materials S2 for cloning information) were transformed into Rosetta *E. coli* cells (Novagen) and plated on LB agar plates (50 μL/mL of carbenicillin and 34 μL/mL of chloramphenicol). Selected colonies were then grown in LB (5 mL, 37 °C, overnight) as a preculture which was added to LB (500 mL) and grown (37 °C) until an $O.D_{600}$ of 0.6. Protein expression was then induced by the addition of IPTG (250 μL of a 1 M stock) and the cultures were further incubated (3 h, 30 °C). The cells were isolated by centrifugation (4000 rpm, 20 min, 4 °C). The cell pellet was resuspended in lysis buffer (50 mM NaH_2PO_4, 300 mM NaCl, 40 mM Imidazole, 1 mM EDTA, pH 8). Cellytic (10x, Sigma) was added, and the solution was incubated (20 min, on ice) and then sonicated (Misonix, ultrasonic cell distruptor, pulsed 5 s on, 5 s off for 5 min). The protein solution was clarified by centrifugation (15 000 rpm, 45 min at 4 °C) and then filtered (Sartorius, 0.2 μm). The protein was purified via affinity purification (GE, Histrap FF, 5 mL, (wash buffer-40 mM Imidazole, 50 mM NaH_2PO_4, 300 mM NaCl, pH 7.4), (elution buffer-500 mM Imidazole, 50 mM NaH_2PO_4, 300 mM NaCl, pH 7.4)). Enterokinase digestion (NEB, 2 μg/mL) was performed to cleave off the peptide tag from the protein of interest followed by a second Histrap [GE, Histrap HP, 5 mL, (wash buffer-50 mM NaH_2PO_4, 300 mM NaCl, pH 7.4), (elution buffer-500 mM Imidazole, 50 mM NaH_2PO_4, 300 mM NaCl, pH 7.4)] to remove the tag from solution. The protein solution was further purified by size exclusion chromatography (GE Hiload 16/60 Superdex, running buffer-50 mM NaH_2PO_4). Each protein was then placed into FlAsH buffer via ultrafiltration (Millipore).

Each purified protein was tested by incubating the protein (200 μL of 0.1 mg/mL) in FlAsH buffer with TCEP (Sigma, final concentration of 3.5 mM), EDT (Sigma, final concentration of 1 mM), and 2-ME (Sigma, final concentration of 1 mM) and left to incubate (2 h, room temperature) followed by the addition of FlAsH-EDT_2 (Invitrogen, final concentration of 0.1 μM, 2 h, room temperature). Each sample was prepared directly into a black Corning 96 well plate which was tested in a PerkinElmer Envision 2101 multilabel plate reader (Ex filter 485 nm, bandwidth 14 nm, Em filter 535 nm, bandwidth 25 nm). Each pure protein was tested six times and reread three times. For the denaturant experiment, each protein was tested as described above, but with the addition of 6 M guanidine, while keeping the protein concentration the same and was incubated for 2 h prior to the addition of TCEP, 2-ME, and EDT.

Analytical Size Exclusion Chromatography (SEC). The samples (0.5 mL of 1 mg/mL) in FlAsH buffer (100 mM Tris-HCl, 100 mM NaCl, 1 mM EDTA, pH 7.8) were injected onto the column (GE Superdex 200 10/300 GL) at 0.5 mL/min with each protein repeated 3 times. The column was calibrated using six proteins as standards (GE Biosystems Calibration Kit). (See SI Figure S7.)

For fluorescent monitoring, samples were prepared by adding to pure protein (0.5 mL of 1 mg/mL) in FlAsH buffer, TCEP (Sigma,

dx.doi.org/10.1021/ja4085034 | J. Am. Chem. Soc. 2013, 135, 16618−16624

final concentration of 3.5 mM), EDT (Sigma, final concentration of 1 mM) and 2-ME (Sigma, final concentration of 1 mM) and incubated (2 h, room temperature). FlAsH-EDT_2 dye was added and incubated in the dark (Invitrogen, final concentration of 0.4 μM, 2 h, room temperature). This sample was desalted (GE, HiTrap 5 mL Desalting column) before injection onto a SEC column (GE Superdex 200 10/300 GL). Samples were taken every 200 μL during the elution and placed into a black Corning 96 well plate. This plate was tested in a PerkinElmer Envision 2101 multilabel plate reader (Ex filter 485 nm bandwidth 14 nm, Em filter 535 nm bandwidth 25 nm). Each purified protein was tested three times with each plate reread three times.

Transmission Electron Microscopy (TEM). TEM was performed on a FEI, Tecnai G^2 20, electron microscope set at 200 KeV. Proteins were immobilized on Formvar/carbon coated 3.05 mm copper grids (TAAB) and negatively stained with 1% Uranyl acetate.[7] Micrographs were analyzed using ImageJ.[41] (See SI Figure S8.)

Circular Dichroism Spectroscopy (CD). The purified proteins were used in FlAsH buffer (100 mM Tris, 100 mM NaCl, 1 mM EDTA, pH 7.8). This experiment was performed on an Applied Photophysics LTD Chirascan spectrometer in a range of 200 to 260 nm with a protein concentration of 0.2 mg/mL with a path length of 0.5 mm. Thermal melts were performed on all purified proteins (0.2 mg/mL in FlAsH buffer) in a range of 4 to 85 °C.[42,43] (See SI Figures S4 and S5 and Table S4.)

Electrospray Mass Spectrometry. Purified proteins were desalted (GE, Hitrap 5 mL Desalting column) and analyzed on a Bruker MaXis mass spectrometer after the addition of 1% Formic acid. (See SI Table S5.)

pH versus GuHCl Measurement. Each purified protein was analyzed by incubating the protein (200 μL of 0.1 mg/mL) in a buffer at the relevant pH (pH 6–7, 100 mM Citrate-phopshate. pH 7.5–8.5 100 mM Tris.HCl) and with the correct concentration of GuHCl, with TCEP (Sigma, final concentration of 3.5 mM), EDT (Sigma, final concentration of 1 mM) and 2-ME (Sigma, final concentration of 1 mM) and incubated (2 h, room temperature) followed by the addition of FlAsH-EDT_2 (Invitrogen, final concentration of 0.1 μM, 2 h, room temperature). Each sample was prepared directly in a black Corning 96 well plate which was scanned in a PerkinElmer Envision 2101 multilabel plate reader (Ex filter 485 nm, bandwidth 14 nm, Em filter 535 nm, bandwidth 25 nm). Each protein was prepared three times separately, and each was reread three times.[44]

■ ASSOCIATED CONTENT

Supporting Information

SDS-PAGE for lysate samples; SDS-PAGE for all purified proteins; as well as TEM, CD, SEC, and electrospray mass spectrometry data for their characterization and sequence alignments and primers used in their manufacture. Raw data for the pH vs GuHCl experiment. This material is available free of charge via the Internet at http://pubs.acs.org.

■ AUTHOR INFORMATION

Corresponding Author

brendan.orner@kcl.ac.uk

Author Contributions

‖These authors contributed equally.

Notes

The authors declare no competing financial interest.

■ ACKNOWLEDGMENTS

We thank E. Hobart, N. Luedtke, Y. Zhang, M. Ardejani, and M. Peczuh for insightful conversations, Fan Rongli for the plasmid coding for WT Dps in pET-32b, and A. T. Phan for the encouragement to perform the experiment in Figure 3. We also thank KCL's Centre for Ultrastructural Imagining and Centre for Biomolecular Spectroscopy for help in characterization of the proteins, D. Thurston's lab for help and access to instrumentation, and J. McDonnell for help with the ESI. T.A.C was sponsored by SINGA and BSE scholarships at NTU and King's respectively and J.F. was supported by CBC's undergraduate research fund. The research at NTU was supported by an SPMS start-up grant, a Singapore Ministry of Education Academic Research Fund Tier 1 Grant (RG 53/06) and B.P.O's personal salary. At KCL, it was supported by start up funds from the School of Biomedical Sciences and a Marie Curie CIG: PCIG13-GA-2013-618538.

■ REFERENCES

(1) Grueninger, D.; Treiber, N.; Ziegler, M. O. P.; Koetter, J. W. A.; Schulze, M.-S.; Schulz, G. E. *Science* **2008**, *319*, 206–209.
(2) Fan, R.; Boyle, A. L.; Cheong, V. V.; Ng, S. L.; Orner, B. P. *Biochemistry* **2009**, *48*, 5623–5630.
(3) Walter, S.; Buchner, J. *Angew. Chem., Int. Ed.* **2002**, *41*, 1098–1113.
(4) Aisen, P.; Listowsky, I. *Annu. Rev. Biochem.* **1980**, *49*, 357–393.
(5) Kis, K.; Volk, R.; Bacher, A. *Biochemistry* **1995**, *34*, 2883–2892.
(6) Homa, F. L.; Brown, J. C. *Rev. Med. Virol.* **1997**, *7*, 107–122.
(7) Fan, R.; Chew, S. W.; Cheong, V. V.; Orner, B. P. *Small* **2010**, *6*, 1483–1487.
(8) Zhang, L.; Swift, J.; Butts, C. A.; Yerubandi, V.; Dmochowski, I. J. *J. Inorg. Biochem.* **2007**, *101*, 1719–1729.
(9) Ueno, T.; Suzuki, M.; Goto, T.; Matsumoto, T.; Nagayama, K.; Watanabe, Y. *Angew. Chem., Int. Ed* **2004**, *43*, 2527–2530.
(10) Kramer, R. M.; Li, C.; Carter, D. C.; Stone, M. O.; Naik, R. R. *J. Am. Chem. Soc.* **2004**, *126*, 13282–13286.
(11) Woersdoerfer, B.; Woycechowsky, K. J.; Hilvert, D. *Science* **2011**, *331*, 589–592.
(12) Keyes, J. D.; Hilton, R. J.; Farrer, J.; Watt, R. K. *J. Nanopart. Res.* **2011**, *13*, 2563–2575.
(13) Qiu, H. J.; Dong, X. C.; Sana, B.; Peng, T.; Paramelle, D.; Chen, P.; Lim, S. *ACS Appl. Mater. Interfaces* **2013**, *5*, 782–787.
(14) Grant, R. A.; Filman, D. J.; Finkel, S. E.; Kolter, R.; Hogle, J. M. *Nat. Struct. Biol.* **1998**, *5*, 294–303.
(15) PDB: 1F33
(16) Ardejani, M. S.; Li, N. X.; Orner, B. P. *Biochemistry* **2011**, *50*, 4029–4037.
(17) Ardejani, M. S.; Chok, X. L.; Foo, C. J.; Orner, B. P. *Chem. Commun.* **2013**, *49*, 3528–3530.
(18) Fletcher, J. M.; Harniman, R. L.; Barnes, F. R. H.; Boyle, A. L.; Collins, A.; Mantell, J.; Sharp, T. H.; Antognozzi, M.; Booth, P. J.; Linden, N.; Miles, M. J.; Sessions, R. B.; Verkade, P.; Woolfson, D. N. *Science* **2013**, *340*, 595–599.
(19) Woolfson, D. N. *Adv. Protein Chem.* **2005**, *70*, 79–112.
(20) Zhang, Y.; Raudah, S.; Teo, H.; Teo, G. W. S.; Fan, R.; Sun, X.; Orner, B. P. *J. Biol. Chem.* **2010**, *285*, 12078–12086.
(21) Zhang, Y.; Fu, J.; Chee, S. Y.; Ang, E. X. W.; Orner, B. P. *Protein Sci.* **2011**, *20*, 1907–1917.
(22) Haile, D. J. *Am. J. Med. Sci.* **1999**, *318*, 230–240.
(23) Harrison, P. M.; Arosio, P. *Biochim. Biophys. Acta, Bioenerg.* **1996**, *1275*, 161–203.
(24) Hintze, K. J.; Theil, E. C. *Cell. Mol. Life Sci.* **2006**, *63*, 591–600.
(25) Leipuviene, R.; Theil, E. C. *Cell. Mol. Life Sci.* **2007**, *64*, 2945–2955.
(26) Theil, E. C. *Annu. Rev. Biochem.* **1987**, *56*, 289–315.
(27) Ilari, A.; Stefanini, S.; Chiancone, E.; Tsernoglou, D. *Nat. Struct. Biol.* **2000**, *7*, 38–43.
(28) Zhang, Y.; Orner, B. P. *Int. J. Mol. Sci.* **2011**, *12*, 5406–5421.
(29) Griffin, B. A.; Adams, S. R.; Tsien, R. Y. *Science* **1998**, *281*, 269–272.
(30) Griffin, B. A.; Adams, S. R.; Jones, J.; Tsien, R. Y. *Methods Enzymol.* **2000**, *327*, 565–578.
(31) Tsien, R. Y. *Annu. Rev. Biochem.* **1998**, *67*, 509–544.

(32) Adams, S. R.; Campbell, R. E.; Gross, L. A.; Martin, B. R.; Walkup, G. K.; Yao, Y.; Llopis, J.; Tsien, R. Y. *J. Am. Chem. Soc.* **2002**, *124*, 6063−6076.
(33) Ignatova, Z.; Gierasch, L. M. *Proc. Natl. Acad. Sci. U. S. A.* **2004**, *101*, 523−528.
(34) Ray-Saha, S.; Schepartz, A. *ChemBioChem* **2010**, *11*, 2089−2091.
(35) Scheck, R. A.; Schepartz, A. *Acc. Chem. Res.* **2011**, *44*, 654−665.
(36) Madani, F.; Lind, J.; Damberg, P.; Adams, S. R.; Tsien, R. Y.; Graslund, A. O. *J. Am. Chem. Soc.* **2009**, *131*, 4613−5.
(37) Luedtke, N. W.; Dexter, R. J.; Fried, D. B.; Schepartz, A. *Nat. Chem. Biol.* **2007**, *3*, 779−784.
(38) Goodman, J. L.; Fried, D. B.; Schepartz, A. *ChemBioChem* **2009**, *10*, 1644−1647.
(39) Scheck, R. A.; Lowder, M. A.; Appelbaum, J. S.; Schepartz, A. *ACS Chem. Biol.* **2012**, *7*, 1367−1376.
(40) Enninga, J.; Mounier, J.; Sansonetti, P.; Van Nhieu, G. T. *Nat. Methods* **2005**, *2*, 959−965.
(41) Schneider, C. A.; Rasband, W. S.; Eliceiri, K. W. *Nat. Methods* **2012**, *9*, 671−675.
(42) Kelly, S. M.; Jess, T. J.; Price, N. C. *Biochim. Biophys. Acta, Proteins Proteomics* **2005**, *1751*, 119−139.
(43) Greenfield, N. J. *Nat. Protoc.* **2006**, *1*, 2876−2890.
(44) Pace, C. N. *Methods Enzymol.* **1986**, *131*, 266−80.